Electronic Supporting Information

Photoresponsive Arylazopyrazole Surfactant/PDADMAC Mixtures: Reversible Control of Bulk and Interfacial Properties

Michael Hardt,[a)] Christian Honnigfort,[a)] Javier Carrascosa-Tejedor,[b,c)] Marius G. Braun,[a)] Samuel Winnall,[b,c)] Dana Glikman,[a)] Philipp Gutfreund,[b)] Richard A. Campbell[c)] and Björn Braunschweig[a)]*

a. Institute of Physical Chemistry and Center of Soft Nanoscience, University of Münster, Corrensstraße 28/30, 48149 Münster, Germany.

b. Institut Laue-Langevin, 71 avenue des Martyrs, CS 20156, 38042 Grenoble Cedex 9, France.

c. Division of Pharmacy & Optometry, University of Manchester, Manchester M13 9PT, United Kingdom.

Corresponding Author Björn Braunschweig, email: braunschweig@uni-muenster.de

Outline

1. Tensiometry results of C_nAAP surfactants and C_nAAP/PDADMAC mixtures

The experimental setup for our pendant drop tensiometer (PAT-1M, Sinterface) is described in detail elsewhere.[1] For tensiometry light intensities of 6.5 mW/cm^2 (Green LED, 525 nm) or 40 mW/cm^2 (UV LED, 365 nm) were used. C_nAAP concentrations that show the most significant interfacial changes in solution were used for the mixtures. Figure S1 presents the differences in equilibrium surface tension between green (E isomer, see Fig. 1 main text) and UV light (Z isomer), where the largest changes are found at concentrations of ~0.1 mM (C_8AAP), ~1 mM (C_4AAP) and ~10 mM (C_0AAP). PDADMAC is known to be surface inactive due to its high solubility in water and, consequently, does not lower the surface tension at the air-water interface (Figure S2).[2] Figures S3 (a) and (b) show the respective dynamic or static surface tension values for the C_nAAP/PDAADMAC mixtures.

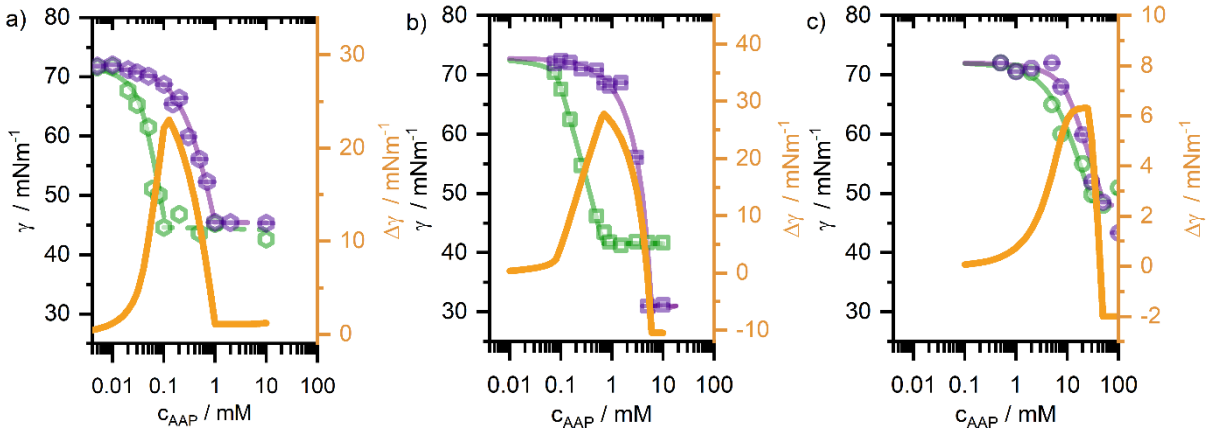

Figure S1: *Equilibrium surface tension of C_nAAP surfactants under green (E isomer) and UV (Z isomer) irradiation for a) C_8AAP, b) C_4AAP, and c) C_0AAP. Orange solid lines indicate the difference in surface tension $\Delta\gamma = \gamma_Z - \gamma_E$ between the different E/Z isomers. The presented surface tensions are reproduced from previous works,[1,3] with permission from ref [1] - Copyright 2023 American Chemical Society and ref [2] with Copyright 2020 Royal Society of Chemistry.*

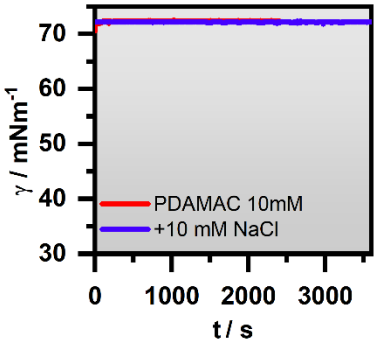

Figure S2: *Dynamic surface tension for a 10 mM PDADMAC solution without surfactants with and without 10 mM NaCl.*

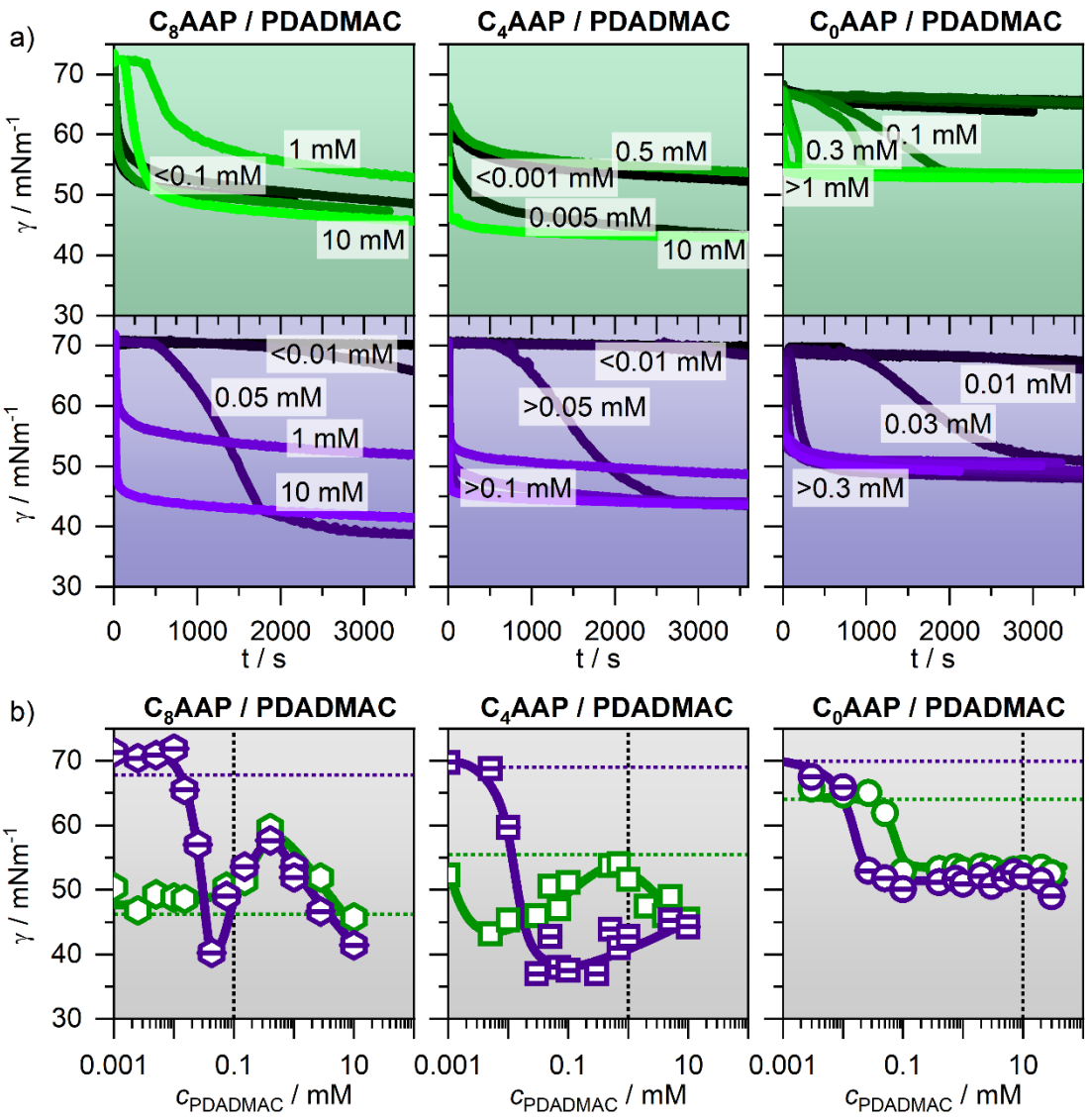

Figure S3: *(a) Dynamic surface tension at the air-water interface for C_nAAP/PDADMAC mixtures with 0.1 mM C_8AAP, 1 mM C_4AAP or respective 10 mM C_0AAP and selected PDADMAC concentrations, which were as indicated in the figure. (b) Equilibrium surface tension at the air-water-interface of C_nAAP/PDADMAC mixtures, which were determined after 1 h. The concentrations of C_nAAP surfactants are marked with vertical lack dashed lines. The colored horizontal dashed lines indicate the surface tension of the surfactants without added PDADMAC.*

2. Neutron reflectometry analysis and model

A similar model for analyzing the neutron reflectometry profiles as was reported in previous studies has been applied but with an additional layer.[4] We refer to the experimental section in the main text for a detailed description of the model that was used to analyze the neutron reflectometry (NR) profiles in our study. The separation of the molecule into a chain and a head part is similar to that described by Honnigfort et al. (Figure S4).[5] Figure S4 shows additionally the structure of the partially deuterated surfactants used for the neutron reflectometry experiments.

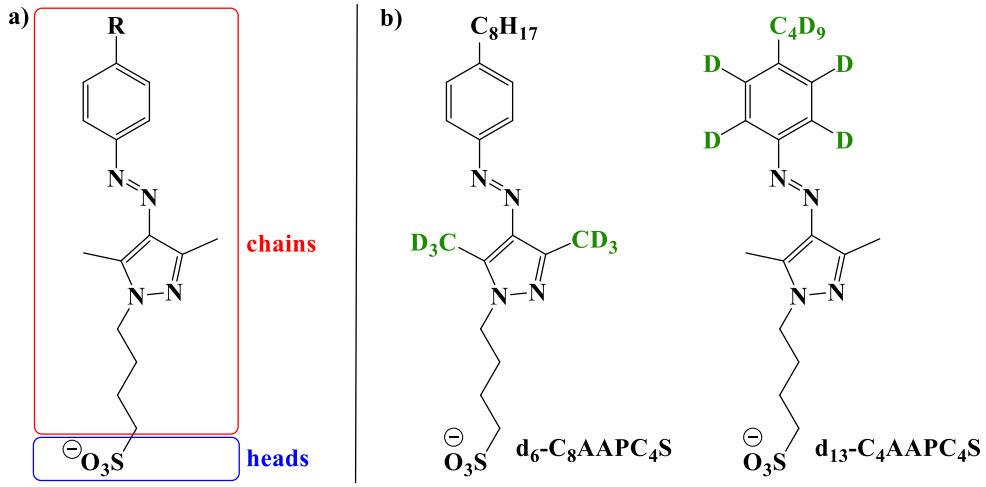

Figure S4: *(a) Scheme of the surfactant and its separation in tails and heads which was applied for the analysis of NR profiles. (b) Presents the structure of the partially deuterated surfactants and their deuteration degree.*

Knowledge of the scattering length densities (SLD) ρ of the individual surfactant and polyelectrolyte parts is necessary to analyze the reflectometry curves. The SLDs are calculated through the scattering length b and the molecular volume V_m:

$$\rho = \frac{b}{V_m} \qquad \text{(EqS1)}$$

Table S1: *Overview of the scattering lengths, molecular volumes and resulting scattering length densities (SLD's) for all subsystem in the P/S mixtures.*

		Scattering length b / fm	Molecular volume V_M / Å^3	SLD ρ / 10^{-6} Å^{-2}
C_4AAP – chains	Hydrogenous	62.76	503.4	1.25
	Deuterated	198.09	503.4	3.94
C_8AAP – chains		121.89	571.4	2.13
Heads		20.26	42.49	4.77
PDADMAC - monomer		2.70	185	0.15

The respective values are listed in Table S1. All NR profiles as well as the corresponding fits to the NR profiles are depicted in Fig. S5 and S6. The fit parameters are listed in Table S2 and S3.

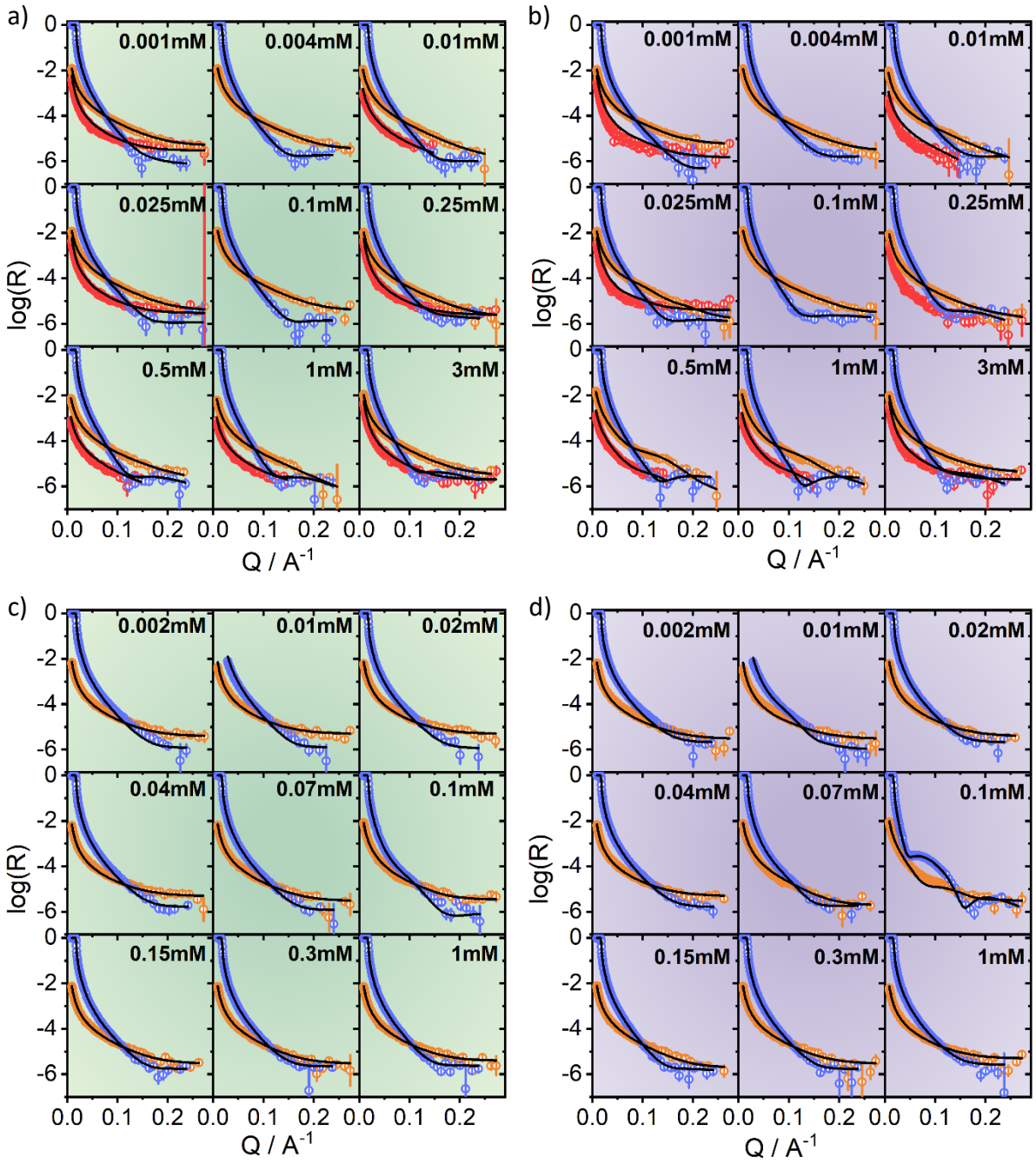

Figure S5*: Neutron reflection profiles for the PDADMAC mixtures with (a), (b) C_4AAP and (c), (d) C_8AAP surfactants under green (a,c) or UV (b,d) irradiation. Three different contrasts were used: deuterated surfactants in D_2O (blue curves), deuterated surfactants in ACMW (orange curves), and hydrogenous surfactants in ACMW (red curves).*

Regarding the physical boundaries, the same amount of surfactant heads and chains need to be realized by fixing the amount of surfactant heads $\Phi_{2,heads}$ to:

$$\Phi_{2,heads} = \frac{V_{m,heads}}{V_{m,chains}} \cdot \frac{d_1}{d_2} \cdot \Phi_{1,chains} \qquad \text{(EqS2)}$$

The surface excesses of the compounds are calculated through the following equation:

$$\Gamma_S = \frac{d_1\Phi_1}{V_{m,chains}\,N_A} + \frac{d_4\Phi_{4,S}}{V_{m,s}\,N_A} \quad \text{(EqS3)}$$

$$\Gamma_P = \frac{d_2\Phi_{2,P}}{V_{m,P}N_A} + \frac{d_3\Phi_{3,P}}{V_{m,P}N_A} \quad \text{(EqS4)}$$

Note that the number of surfactants in layer 2 (head parts) corresponds to the number in layer 1 (chain parts). Therefore, the number of surfactants in layer 2 does not increase the total amount of surfactants and has no contribution to Γ_S.

Table S2: *Results and parameters for the structure of d_{13}-C_4AAP/PDADMAC mixtures at the air-water interface from NR profiles under green (E) and UV (Z) irradiation (text color). The C_nAAP concentration has been kept constant, as stated in the main text. The PDADMAC-concentration c_{Poly} is displayed below. The parameters for the fit were each layer's thickness d_i and composition (described as volume fraction) Φ_i .*

c_{Poly} / mM	Chi^2	d_1 / Å	Φ_1 chains/%	d_2 / Å	Φ_2 heads/%	Φ_2 poly/%	d_3 / Å	Φ_3 poly/%	d_4 / Å	Φ_4 surf /%
0.001	38.4	15.6±0.4	90	6±3	20	0±10	8±4	12±6	-	-
0.004	3.2	15.7±0.2	90	4±1	30	35±5	71±34	0.7±0.5	-	-
0.01	14.8	15.4±0.3	90	4±1	29	16±12	9±5	7±4	-	-
0.025	36.9	16.0±0.4	90	6±3	20	0±7	180±77	2±4	-	-
0.1	6.7	15.7±0.2	90	5±1	26	29±5	137±55	0.8±0.5	-	-
0.25	17.0	13.8±0.3	90	6±2	17	3±7	5±1	32±6	-	-
0.5	17.1	12.7±0.3	90	6±2	16	0±10	6±1	65±7	-	-
1	11.3	12.2±0.2	90	6±1	15	0±9	7±1	57±5	-	-
3	19.8	13.6±0.3	90	6±1	17	0±10	8±1	57±5	-	-
0.001	70.8	14.2±0.6	90	6±3	18	7±13	30[a]	1±3	26	2±4
0.004	3.5	15.3±0.2	90	4±1	29	0±4	60±41	0.6±0.5	-	-
0.01	38.8	13.0±0.5	90	6±2	16	24±13	30±30[b]	0.4±2	-	-
0.025	70.9	14.2±0.6	90	6±3	18	27±20	30[a]	5±3	26	3±4
0.1	2.5	15.5±0.1	90	4±1	29	71±5	15±1	9±1	26	2±1
0.25	31.1	11.1±0.4	90	6±2	14	0±11	10±1	47±5	-	-
0.5	34.1	15.2±0.4	90	5±1	23	72±21	18±5	7±3	27	9±2
1	24.1	14.2±0.3	90	6±1	18	80±15	25±10	4±2	26	5±2
3	41.3	12.4±0.5	90	6±2	16	0±13	10±1	42±6	-	-

[a] *These values were fixed to 30 Å as too high polymer ratios were calculated that resulted in unsteady fit curves.*
[b] *This value has an assumed error of itself because no value was found that caused a Chi^2 increase of 5%.*

Table S3: *Results and parameters for the d_6-C_8AAP/PDADMAC mixture. For simplicity, we refer for the explanation of the abbreviated parameters to Table S1 and the main text.*

c_{Poly} / mM	Chi²	d_1 / Å	Φ_1 chains/%	d_2 / Å	Φ_2 heads/%	Φ_2 poly/%	d_3 / Å	Φ_3 poly/%	d_4 / Å	Φ_4 surf /%
0.002	38.5	16.0±0.6	90	4±1	27	0±3	-	-	-	-
0.01	90.4	15.3±0.9	90	4±2	26	34±34	-	-	-	-
0.02	38.1	15.4±0.6	90	4±1	26	0±3	-	-	-	-
0.04	25.0	15.4±0.5	90	4±1	26	0±2	-	-	-	-
0.07	12.3	15.9±0.4	90	4±1	27	0±2	-	-	-	-
0.1	6.6	17.7±0.3	90	6±1	20	0±1	45±3	9±1	-	-
0.15	3.2	16.7±0.3	90	4±1	28	7±6	45±7	2±1	-	-
0.3	3.0	16.7±0.2	90	4±1	28	0±3	73±27	0.6±0.4	-	-
1	4.3	16.3±0.3	90	4±1	27	38±8	66±34	0.6±0.5	-	-
0.002	47.2	14.3±0.6	90	4±1	24	0±3	-	-	-	-
0.01	109.8	14.2±1.0	90	4±2	24	16±28	-[a]	-[a]	-	-
0.02	8.8	15.4±0.3	90	4±1	26	0±5	58±20	1.0±0.7	-	-
0.04	10.3	15.3±0.4	90	4±1	26	0±2	-	-	-	-
0.07	14.7	18.0±0.4	90	6±1	20	0±2	52±6	4±1	-	-
0.1	40.0	16.2±0.6	90	6±1	18	0±7	43±1	83±1	-	-
0.15	3.5	16.4±0.2	90	4±1	27	73±8	45±22	0.8±0.4	-	-
0.3	3.0	16.3±0.2	90	4±1	27	13±6	48±19	0.7±0.4	-	-
1	6.4	15.9±0.3	90	4±1	27	0±8	98±98[b]	0.4±0.8	-	-

[a] *The use of a layer 3 was omitted as the necessary cut of the low-Q data caused artefacts in the fit.*
[b] *This value has an assumed error of itself because no value was found that caused a Chi² increase of 5%.*

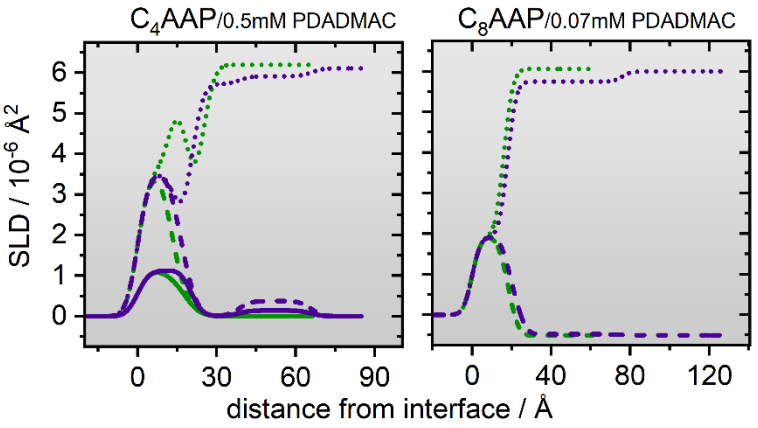

Figure S6*: Selected SLD profiles for the C_nAAP/PDADMAC mixtures with PDADMAC concentration as stated above. The straight lines represent the h-surfactants in ACMW, the dashed lines the d-surfactants in ACMW and the dotted lines the d-surfactants in D_2O. The irradiation type is indicated by the color of the lines.*

3. Turbidity of C_nAAP / PDADMAC mixtures in bulk aqueous solutions

Aggregates of the C_4AAP/PDADMAC and C_8AAP/PDADMAC mixtures exhibit reversible changes between E and Z isomers on for their electrophoretic mobility but not for the particle size, while changes for both of the latter are reversible for C_0AAP/PDADMAC mixtures. The lack of a possible re-dissolution of these aggregates is also visible in the samples' turbidity (Figure S7). Qualitatively, the change in the turbidity of the sample can be seen by the bare eye. A more quantitative approach is shown by the absorbance of the mixture at 700 nm since, in this spectral region, the increased absorbance mainly originates from the turbidity of the sample.

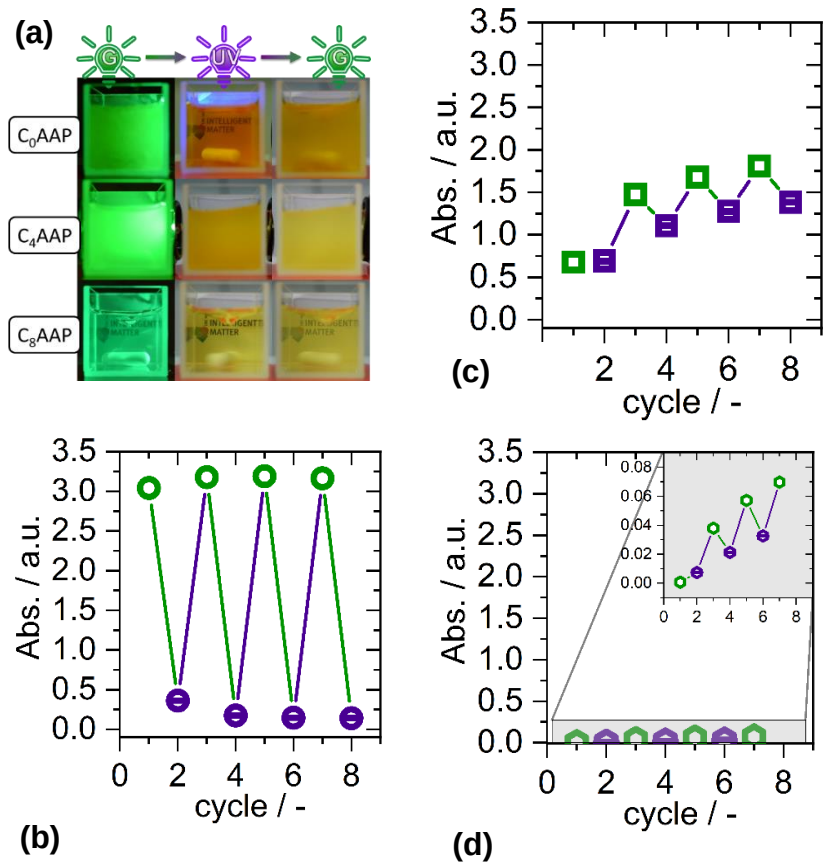

Figure S7. *Turbidity changes of C_nAAP/PDADMAC mixtures. (a) Photographs of sample solutions for a switching cycle of the light irradiation as indicated in the top part. (b), (c) and (d) changes in absorbance of the C_nAAP/PDADMAC mixture at a wavelength of 700 nm. Circles (b) represent mixtures with C_0AAP, squares with C_4AAP (c) and hexagons (d) with C_8AAP surfactants. For the C_8AAP mixture, an inset with a different scale is shown. The irradiation type is illustrated as green, empty or respective violet, horizontal lined symbols. The mixing ratio was fixed for all systems to equimolar concentrations in order to achieve maximum turbidity.*

4. UV\Vis spectra of E and Z isomers

We have done UV\VIS spectroscopy to give at least an approximate on the PSS of the surfactants. The results are now shown in Figure S8 of the ESI and are reproduced below. We observe (i) minor changes in the spectra of the E isomers which are likely due caused by aggregation with PDADMAC and (ii) massive changes of the $\pi \rightarrow \pi^*$ (~320 nm) and $n \rightarrow \pi^*$ (~420 nm) bands. These changes indicate that the samples are dominated either by the E (irradiation with 520 nm green light) or the Z isomer (irradiation with UV light).

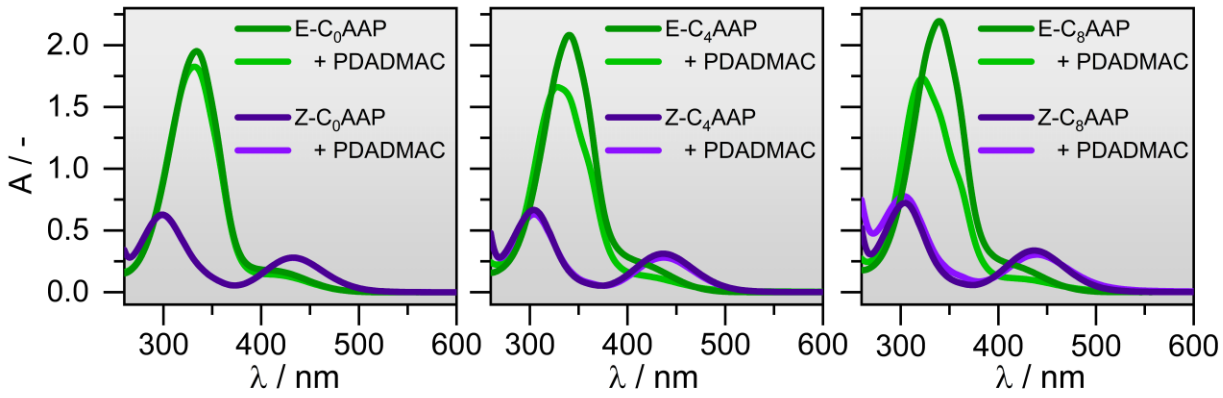

Figure S8. *UV\VIS spectra of 0.1 mM C_0AAP, 0.1 mM C_4AAP and 0.1 mM C_8APP in their E and Z states and UV\Vis spectra of their corresponding mixtures with 0.1 mM PDADMAC.*

5. Electrophoretic mobilities and hydrodynamic diameters of C_nAAP/PDADMAC aggregates

Figure S10 extends Figure 3 (main text) by several different mixing ratios. As in the main text, the aggregate charges but not the particle sizes can be nearly reversibly switched for C_4AAP and C_4AAP mixtures. For the C_0AAP mixtures, reversible changes in particle sizes are seen except for the lowest PDADMAC concentrations, as the aggregate charges are low under both irradiation types. In Figure S9, the results from the individual surfactants (Figure 2, main text) are divided into separate diagrams, which enables a direct comparison of the PDADMAC/C_nAAP mixtures with the surfactants in either the E or Z configuration.

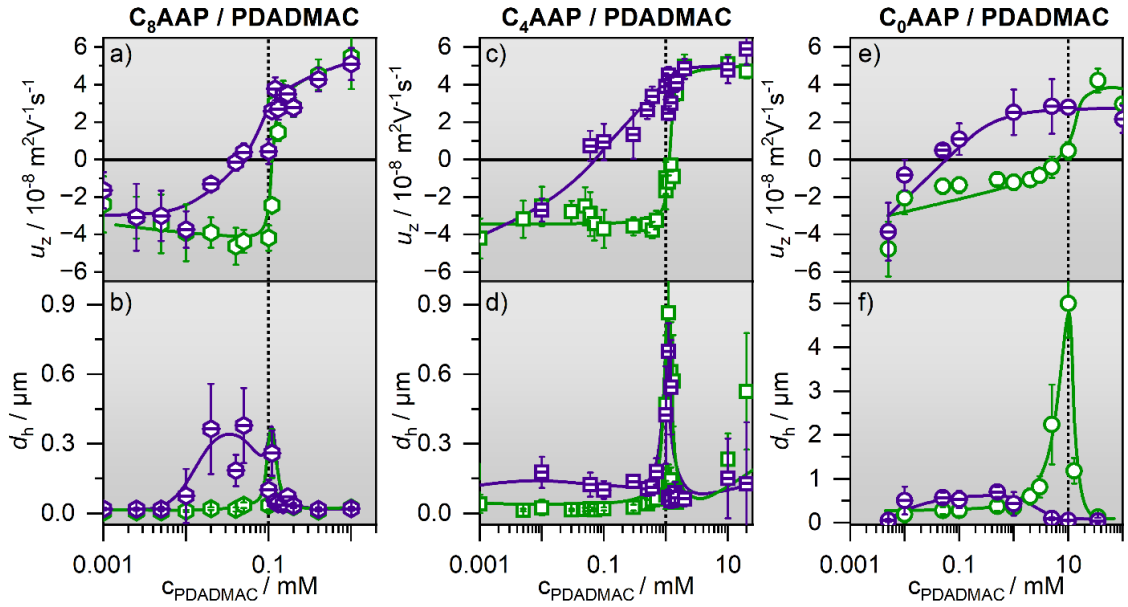

Figure S9. *Electrophoretic mobilities u_ζ (a,c,e) and hydrodynamic diameters d_h (b,d,f) of each PDADMAC/C_nAAP mixture at a fixed surfactant concentration of 10 mM (C_0AAP), 1 mM (C_4AAP) or 0.1 mM (C_8AAP). The irradiation type is illustrated as green, empty or respective violet, horizontal lined symbols.*

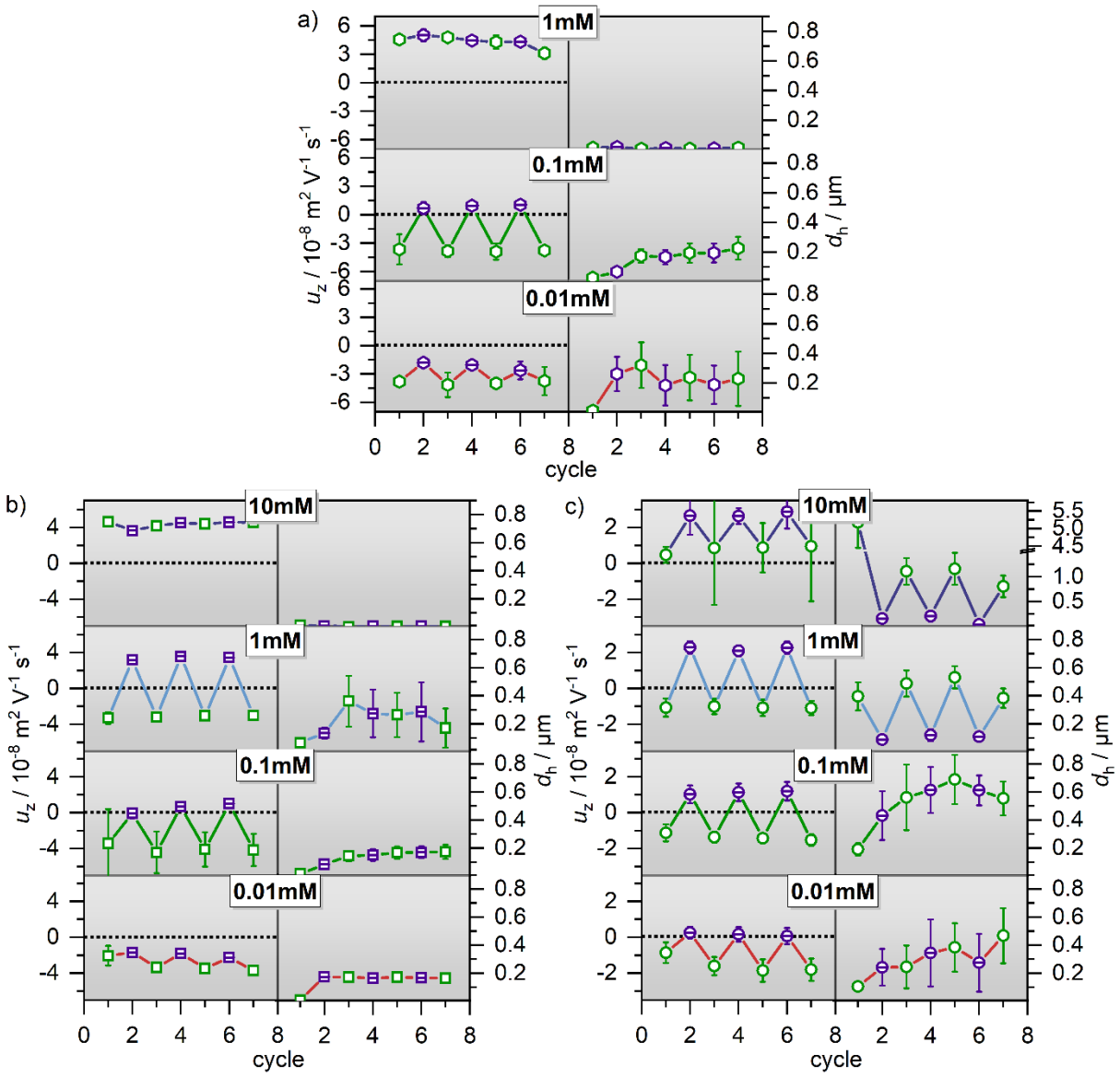

Figure S10. *Electrophoretic mobilities u_ζ and hydrodynamic diameters d_h after several green/UV irradiation cycles for PDADMAC mixtures with a) 0.1 mM C_8AAP, b) 1 mM C_4AAP c) 10 mM C_0AAP with the PDADMAC concentration as is indicated in the figure. The irradiation type is indicated as green, empty symbols or respective violet, horizontal lined symbols.*

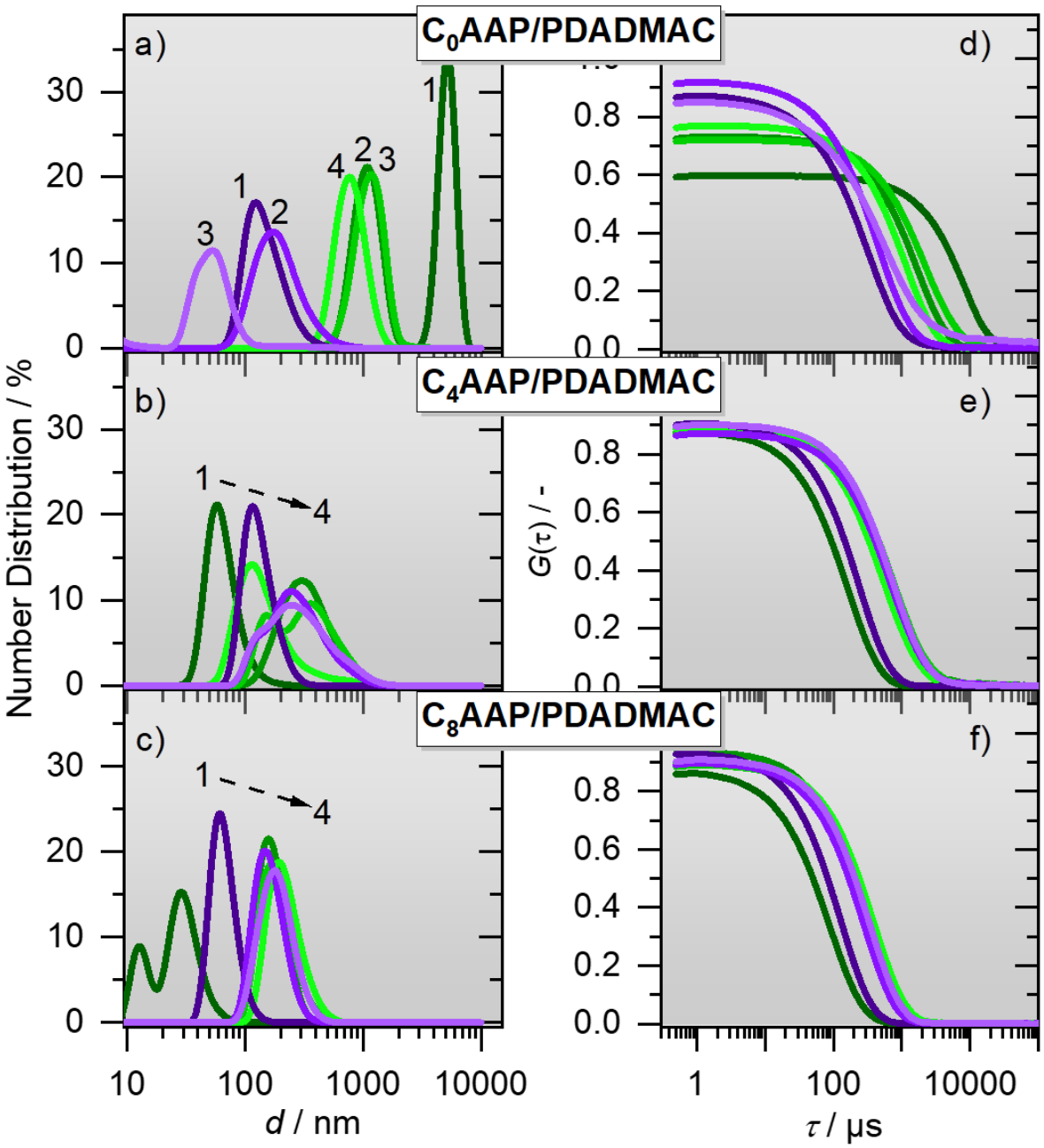

Figure S11: *Number-weighted particle size distributions of (a) C_0AAP, (b) C_4AAP and (c) C_8AAP mixtures with PDADMAC for different switching cycles starting with green (dark green line indicated by "1") , then switching to UV light (dark blue for the first cycle indicated by "1"). (d), (e) and (f) present the autocorrelation functions of C_0AAP, C_4AAP and C_8AAP mixtures with PDADMAC, respectively. Color coding in (d)-(f) is identical to (a)-(c). The PDADMAC concentrations equal the mixtures in Fig. 3 in the main text.*

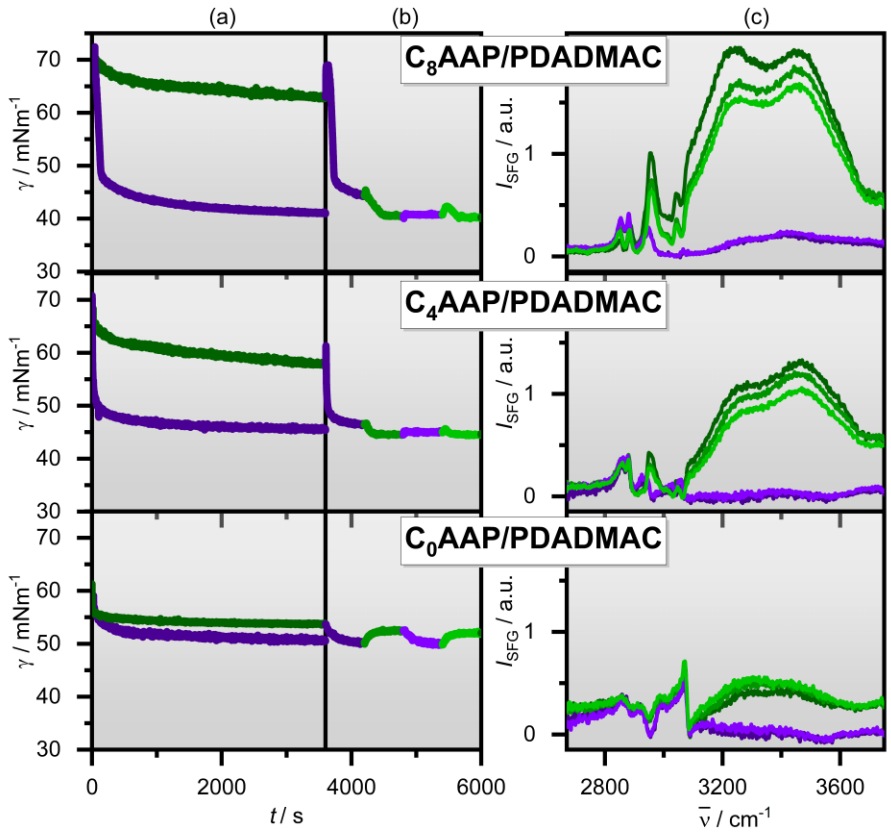

Figure S12: *Interfacial properties of C_nAAP/PDADMAC mixtures upon E/Z photo-isomerization from surface tensiometry (a) and (b) as well as from SFG spectroscopy (c). We show the surface tension and SFG spectra for different E/Z switching cycles indicated by the different colors in the figure. For that, we have used PDADMAC concentrations of 0.1mM, 0.7mM, and 7mM mixed with 0.1 mM C_8AAP, 1 mM C_4AAP and 10 mM C_0AAP, respectively. For (a), samples were first irradiated 1 h with either green or UV light followed by (b) E/Z switching cycles with a period of 10 min each, which were done after equilibration under irradiation with green light. (c) shows SFG spectra of mixtures at the air-water after 1 h equilibration under green irradiation and for subsequent E/Z switching cycles with a period of 10 min. Here the dark green is the first and the SFG spectrum in light green color was taken after the last cycle.*

6. Supporting Details on Vibrational Sum-Frequency Generation (SFG)

Details about the SFG setup can be found elsewhere.[6] The fitting procedure has been reported previously and will be discussed here only shortly.[7] SFG spectra were fitted based on eqn. (EqS5) using a combination of a non-resonant contribution, Lorentzian profiles for the C–H modes and Voigt profiles for the inhomogeneously broadened O–H vibrational modes:

$$X_{eff}^{(2)} = X_{NR}^{(2)} + \sum_k \frac{A_k e^{i\,\phi_k}}{\omega_{IR} - \omega_k + i\gamma_k} + \sum_q \frac{A_q e^{i\phi_q}}{\sqrt{2\pi\sigma_q}} \int_{-\infty}^{\infty} \frac{\exp\left(-\frac{\left(\omega'_q - \omega_q^0\right)^2}{2\sigma_q^2}\right)}{\omega_{IR} - \omega'_q + i\gamma_q}\, d\omega'_q \qquad \text{(EqS5)}$$

Table S4. *Exemplary fit parameter from the analysis of SFG spectra. PDADMAC concentrations in the mixtures were 0.075 mM for mixtures with C_8AAP, 0.9 mM C_4AAP and 7 mM C_0AAP.*

		C_8AAP/PDADMAC		C_4AAP/PDADMAC		C_0AAP/PDADMAC	
X'_{NR}		0.28 ±0.01	0.23 ±0.01	0.34 ±0.01	0.27 ±0.01	0.80 ±0.01	0.70 ±0.02
d^+	A_k / a.u	0.04 ±0.04	0.25 ±0.03	0.23 ±0.05	0.17 ±0.05	0.07 ±0.03	0.07 ±0.03
	Γ_k / cm^{-1}	5	5.2	5	5	8	8
	ϕ / π	1	1	1	1	1	1
	ω_k / cm^{-1}	2857	2857	2857	2857	2856	2856
r^+	A_k / a.u	0.52 ±0.03	0.29 ±0.02	0.3 ±0.03	0.36 ±0.01	0.10 ±0.03	0.14 ±0.03
	Γ_k / cm^{-1}	12	12	10	10	7	7
	ϕ / π	1	1	1	1	1	1
	ω_k / cm^{-1}	2886	2886	2888	2888	2878	2878
r^- / r^+_{FR}	A_k / a.u	1.00 ±0.01	0.49 ±0.01	0.39 ±0.01	0.30 ±0.01	0.09 ±0.02	0.07 ±0.02
	Γ_k / cm^{-1}	24	24	16	23	14	14
	ϕ / π	1	1	1	1	0	0
	ω_k / cm^{-1}	2940	2940	2947	2947	2972	2972
arom. C–H	A_k / a.u	0.24 ±0.03	0.03 ±0.05	0.15 ±0.03	0.10 ±0.03	0.00 ±0.02	0.00 ±0.02
	Γ_k / cm^{-1}	6	6	9	9	15	15
	ϕ / π	1	1	1	1	1	1
	ω_k / cm^{-1}	3033	3033	3033	3033	3019	3019
arom. C–H	A_k / a.u	0.27 ±0.02	0.19 ±0.03	0.08 ±0.04	0.20 ±0.03	0.84 ±0.03	0.62 ±0.03
	Γ_k / cm^{-1}	12	12	10	10	8	8
	ϕ / π	1	1	1	1	1	1
	ω_k / cm^{-1}	3067	3067	3069	3069	3070	3070
OH_1	A_q / a.u	110.9 ±0.6	39.8 ±0.4	55.4 ±0.5	1 ±1	35.2 ±0.9	3 ±1
	σ_q / cm^{-1}	98	98	98	98	120	120
	ϕ / π	0	0	0	0	0	1
	ω_q^0 / cm^{-1}	3237	3237	3231	3231	3203	3203
OH_2	A_q / a.u	94.7 ±0.9	25.8 ±0.8	59 ±1	0 ±1	5.8 ±0.7	12 ±1
	σ_q / cm^{-1}	102	102	126	126	120	120
	ϕ / π	0	0	0	0	0	1
	ω_q^0 / cm^{-1}	3434	3434	3440	3440	3434	3434
$OH_{D.}$	A_k / a.u	0.00 ±0.02	0.06 ±0.01	0.00 ±0.01	0.00 ±0.02	0.00 ±0.02	0.04 ±0.02
	Γ_k / cm^{-1}	47	47	47	29	47	50
	ϕ / π	0	0	0	0	0	0
	ω_k / cm^{-1}	3710	3710	3710	3720	3710	3705

The Lorentzian line shape of the k[th] mode is described through the amplitude A_k, the phase ϕ_k, the resonance frequency ω_k and the bandwidth γ_k. The Voigt profile is a convolution of a Lorentzian and a Gaussian distribution. It is defined through the aforementioned parameters of the q[th] vibrational modes (A_q, ϕ_q, ω_q and γ_q) plus the width of the Gaussian profile (FMHM = $\sqrt{2\ln(2)}\,\sigma_q$). To keep the number of free parameters low, in most cases only the amplitudes of the relevant vibrational bands were changed as the only free parameter after finding an optimal set of parameters. For some mixtures, the phase of the O–H modes had to be changed for high PDADMAC concentrations that implicate a charge reversal at the interface. Table S4 shows some exemplary parameter sets of the fits. The results of the fits with all SFG spectra are shown in Figure S13.

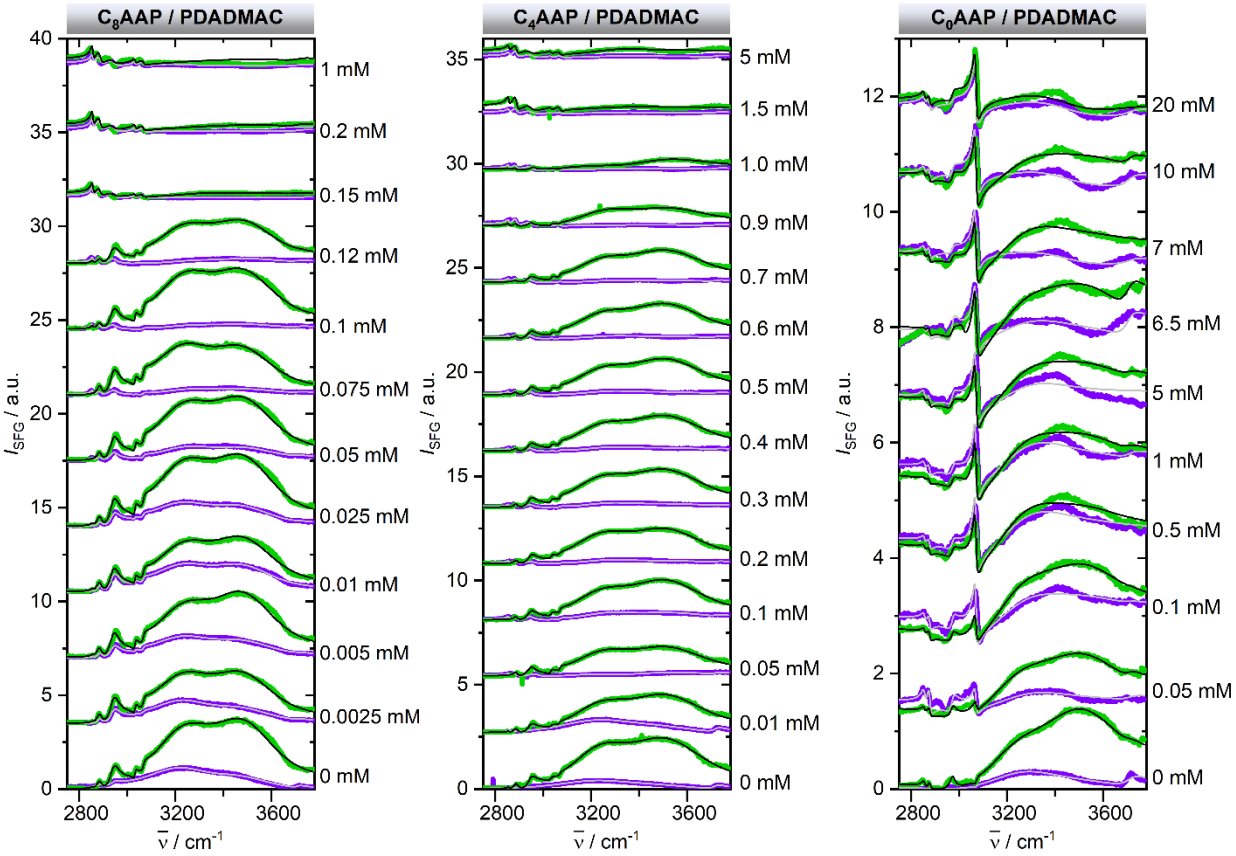

Figure S13: *SFG spectra of C_nAAP/PDADMAC mixtures in showing CH and OH stretching bands from interfacial molecules. Fits to the spectra according to equation EqS5 are shown in black (green irradiation) and grey (UV irradiation).*

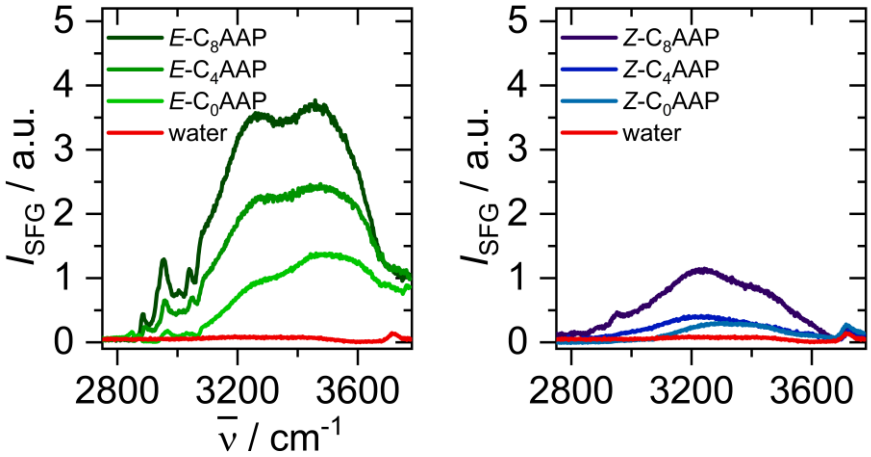

Figure S14: *SFG spectra of air-water interfaces with C_nAAP surfactants in their E and Z configurations and the spectrum of the neat air/water interface. The C_nAAP concentrations were 0.1 mM, 1 mM and 10 mM for C_8AAP, C_4AAP and C_0AAP surfactants respectively. See main text for the relevance for these concentrations.*

7. Supporting Information on the measurement of foam stability

Stability of aqueous foams from P/S mixtures was determined with a dynamic foam analyzer DFA100 (*Krüss*, Germany). The device was in an enclosed chamber to avoid irradiation by ambient light and equipped by 365 nm and 520 nm LEDs for continuous in situ irradiation of the aqueous solution for at least 20 min before foam formation. For that 55 mL sample solution was filled in a glass column with a length of 250 mm length and a diameter of 40 mm and a porous glass frit (Duran, 50 mm diameter, pore size 3 (16-40 µm), *Rettberg*, Germany) at the bottom. Prior to foam formation all solutions were irradiated inside the foam column with either 365 nm or 520 nm light for at least 20 min and, subsequently, ambient air with a gas flow of 0.6 l/min was passed through the frit until a total height of ~180mm was achieved. After foam formation was complete, the foam height was continuously monitored as a function of time using the light transmission through the foam column, for that we have used an infrared LED column which avoids unintentional switching of the surfactants that can be caused by applied the optical measurement of the foam height.

8. References

1 M. Hardt, F. Busse, S. Raschke, C. Honnigfort, J. Carrascosa-Tejedor, P. Wenk, P. Gutfreund, R. A. Campbell, A. Heuer and B. Braunschweig, *Langmuir*, 2023, **39**, 5861–5871.

2 D. Hu and K. C. Chou, *J. Am. Chem. Soc.*, 2014, **136**, 15114–15117.

3 C. Honnigfort, R. A. Campbell, J. Droste, P. Gutfreund, M. R. Hansen, B. J. Ravoo and B. Braunschweig, *Chem. Sci.*, 2020, **11**, 2085–2092.

4 M. Schnurbus, M. Hardt, P. Steinforth, J. Carrascosa-Tejedor, S. Winnall, P. Gutfreund, M. Schönhoff, R. A. Campbell and B. Braunschweig, *ACS Appl. Mat. & Int.*, 2022, **14**, 4656–4667.
5 C. Honnigfort, R. A. Campbell, J. Droste, P. Gutfreund, M. R. Hansen, B. J. Ravoo and B. Braunschweig, *Chem. Sci.*, 2020, **11**, 2085–2092.
6 N. García Rey, E. Weißenborn, F. Schulze-Zachau, G. Gochev and B. Braunschweig, *J. Phys. Chem. C*, 2019, **123**, 1279–1286.
7 M. Schnurbus, M. Hardt, P. Steinforth, J. Carrascosa-Tejedor, S. Winnall, P. Gutfreund, M. Schönhoff, R. A. Campbell and B. Braunschweig, *ACS App. Mat. Int.*, 2022, **14**, 4656–4667.